Enhanced localized energetic ion losses resulting from first-orbit linear and non-linear interactions with Alfvén eigenmodes in DIII-D

X. Chen, W. W. Heidbrink, G. J. Kramer, M. A. Van Zeeland, D. C. Pace, C. C. Petty, R. K. Fisher, R. Nazikian, L. Zeng, M. E. Austin, B. A. Grierson, and M. Podesta

---

Enhanced localized energetic ion losses resulting from first-orbit linear and non-linear interactions with Alfvén eigenmodes in DIII-D[a]

X. Chen,[1,2,b] W. W. Heidbrink,[1] G. J. Kramer,[3] M. A. Van Zeeland,[2] D. C. Pace,[2] C. C. Petty,[2] R. K. Fisher,[2] R. Nazikian,[3] L. Zeng,[4] M. E. Austin,[5] B. A. Grierson,[3] and M. Podesta[3]

[1]*University of California-Irvine, Irvine, California 92697, USA*
[2]*General Atomics, P.O. Box 85608, San Diego, California 92186, USA*
[3]*Princeton Plasma Physics Laboratory, P.O. Box 451, Princeton, New Jersey 08543, USA*
[4]*University of California, Los Angeles 90095, California, USA*
[5]*University of Texas-Austin, Austin, Texas 78712, USA*

Two key insights into interactions between Alfvén eigenmodes (AEs) and energetic particles in the plasma core are gained from measurements and modeling of first-orbit beam-ion loss in DIII-D. First, the neutral beam-ion first-orbit losses are enhanced by AEs and a single AE can cause large fast-ion displacement. The coherent losses are from born trapped full energy beam-ions being non-resonantly scattered by AEs onto loss orbits within their first poloidal transit. The loss amplitudes scale linearly with the mode amplitude but the slope is different for different modes. The radial displacement of fast-ions by individual AEs can be directly inferred from the measurements. Second, oscillations in the beam-ion first-orbit losses are observed at the sum, difference, and harmonic frequencies of two independent AEs. These oscillations are not plasma modes and are absent in magnetic, density, and temperature fluctuations. The origin of the non-linearity as a wave-particle coupling is confirmed through bi-coherence analysis, which is clearly observed because the coherences are preserved by the first-orbit loss mechanism. An analytic model and full orbit simulations show that the non-linear features seen in the loss signal can be explained by a non-linear interaction between the fast ions and the two independent AEs. © 2014 AIP Publishing LLC. [http://dx.doi.org/10.1063/1.4891442]

I. INTRODUCTION

Energetic particles (EPs) such as α-particles produced by fusion reactions, fast ions from neutral beam injection (NBI), and ion cyclotron heating play an important role in plasma heating and current drive. Large energetic-particle populations can also drive plasma instabilities, for example, Alfvén eigenmodes (AEs). The AEs are capable of redistributing the EP population and expelling energetic particles before they transfer their energy to the bulk plasma.[1,2] Multiple Alfvén eigenmodes are often observed in magnetically confined plasmas[2–4] and coherent fast-ion transport/losses are also commonly observed.[5–9] AEs are predicted to be unstable in ITER[10] and have the potential to cause significant α-particle transport in burning plasmas.[11] The avoidance of damage to plasma facing components due to concentrated EP loss is an important issue for ITER; therefore, understanding the interactions between AEs and fast ions in present devices and developing and validating theories and numerical models is important for mitigating the deleterious effects of AEs and even for controlling them in a favorable way in ITER and future burning plasma devices.

This paper presents insights into AE-EP interaction gained from the measurements and modeling of first-(poloidal-)orbit

beam-ion losses induced by toroidal Alfvén eigenmodes (TAEs)[12–14] and reversed shear Alfvén eigenmodes (RSAEs)[15–17] on the DIII-D tokamak. These particles are non-resonantly scattered by AEs and detected by the fast-ion loss detectors (FILDs)[18,19] located on the machine wall. The edge loss measurements carry important information about AE-EP interactions in the plasma core.

The first-orbit loss mechanism allows unique and quantitative measurement of radial displacement of fast ions due to individual modes. Large (∼10 cm) radial displacement by a single mode is measured and enables experimental validation of numerical codes. The observation of enhanced concentrated loss at the detector through this loss channel suggests its potential harm to the device wall components. In addition, this observation has inspired a new diagnostic application—the "light-ion beam probe" (LIBP)—which can be used to probe core modes and three-dimensional field effects. Summary of results that were first reported in Ref. 20 and then detailed in Ref. 21 will be given in Sec. II, along with new data obtained from specially designed experiments.

The first-orbit loss mechanism also allows a new non-linear feature observed in the fast ion loss signals— oscillations at sum, difference, and harmonic frequencies of multiple independent AEs. The data are understood with the aid of an analytical model and numerical simulations. The non-linearity is not generated by the wave-wave coupling but by the non-linear coupling of particle orbital responses to

multiple waves. Although the loss measurement is of non-resonant, barely confined ions, it is likely that similar processes occur for well-confined, resonant fast ions.[22] Details on results beyond those reported in Ref. 23 are presented in Sec. III.

The AE-EP experiments presented in this paper are conducted on the DIII-D tokamak. The DIII-D tokamak has major radius $R \sim 170$ cm and minor radius $r \sim 63$ cm. Figure 1 shows the elevation of the tokamak overlaid with a typical inner-wall limited (IWL) plasma equilibrium flux surfaces reconstructed by EFIT[24] and key diagnostics used in this study. The core mode activity is measured by CO_2 interferometer chords (one radial and three vertical)[25] and forty electron-cyclotron-emission (ECE) radiometer channels.[26] The density profile is monitored with Thomson scattering[27] (not shown) and a high-resolution reflectometer.[28] The fast-ion density profile is measured by fast-ion Dα (FIDA) spectroscopes.[29] (Only the vertical viewing system is shown.) Poloidal and toroidal magnetic coil arrays (not shown) provide information about the poloidal (m) and toroidal (n) mode numbers of the AEs. The fast-ion loss measurements are obtained from the FILD1 (below mid-plane) and FILD2

(near mid-plane). FILD is a scintillator based magnetic spectrometer. Its camera data (up to 160 frames per second) resolve the energy and pitch angle of energetic ions that reach its position on the outer wall, while its photomultiplier (PMT) data resolve frequency information up to 500 kHz.

II. FAST-ION FIRST-ORBIT LOSS THROUGH LINEAR INTERACTIONS WITH ALFVÉN EIGENMODES

A. Summary of previous results

Prompt neutral beam-ion losses driven by TAEs and RSAEs have been observed on DIII-D. The detected coherent losses are of full-energy beam ions and emerge quickly following the beam turn on (<0.1 ms, consistent with a single poloidal transit period). Losses coincide with different beams that are displaced toroidally around the machine as the q-profile evolves. To better understand the loss process, a series of simulations are carried out. The ideal MHD mode solver NOVA[30] code has been applied to calculate the AEs, where an eigenmode is identified by comparing the measured and simulated radial temperature fluctuation profiles and then scaled to match the measured amplitude.[31] Wave-particle interactions are calculated with the full-orbit following SPIRAL code[32] which uses inputs such as the EFIT reconstructed plasma equilibria that are constrained by motional Stark effect (MSE) measurements,[33] the eigenmodes calculated by NOVA, the TRANSP/NUBEAM[34,35] predicted beam birth profiles with the addition of scrape-off layer ionization as calculated by an IDL beam deposition calculation code,[36] and a realistic machine wall model. Both pitch angle scattering and slowing down effects are included. Forward and reverse (which has better statistics) tracking are performed in both Monte-Carlo and single particle computations. Simulations reproduce many experimental observations, such as good overlay between reverse-tracked lost particles and the birth profile of the experimentally identified neutral-beam source in space and velocity, and the fast rise/decay of the loss signal relative to the switch on/off of the relevant beam. It is found that the observed losses are dominated by non-resonant trapped ions born on orbits that would, in the absence of MHD activity, carry them close to (but not incident on) the FILD after one poloidal bounce. In the presence of AEs, they are scattered onto orbits that can intersect the FILD before completing their first drift-orbit (referred as perturbed orbit from now on). This differs from typical coherent-loss measurements, where particles are lost after many circuits around the torus. The AE-induced loss occurs on such a short time scale (within one poloidal transit) that the particles only interact with the mode once; therefore, a resonance is not required for a particle to gain/lose non-zero energy or pitch scattering from the wave and be lost. Unlike the conventional coherent loss that rotates with the mode, thereby spreading the heat load over a large area, the AE-induced prompt loss is localized to the wall due to its first-orbit loss characteristic and affects more particles due to its non-resonant loss characteristic. Enhanced (nearly doubled) FILD loss is observed in some discharges and the AE-induced prompt loss can count for a large fraction of the total detected loss at FILD. It suggests this loss channel can
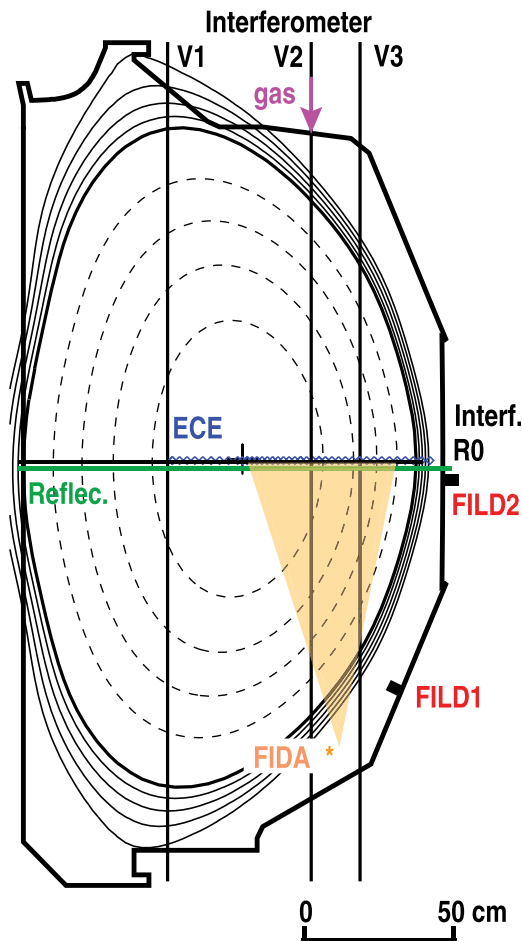

FIG. 1. Elevation of the DIII-D tokamak. Typical IWL shape plasma equilibrium flux surfaced (the thicker solid line indicates the last close flux surface) overlaid with three vertical (V1, V2, and V3) and radial (R0) CO_2 interferometers, gas valve (its port location is at the same poloidal angle as V2 interferometer), 40 ECE channels (blue diamonds), reflectometer (green solid line along midplane), viewing chords of the vertical FIDA system (orange shaded region), and two fast ion loss detectors–FILD1 and FILD2.

introduce new, unexpected localized heat load on the vessel wall.

The prompt coherent loss process is also studied using an orbital topology map.[37] By placing the start and end of one perturbed single particle orbit [Fig. 13 in Ref. 21], it is readily apparent that the particle is born as a trapped confined particle, but then is pushed across the loss boundary by the AE and lost to the FILD.

The AE-induced prompt beam-ion loss has been observed on both FILDs for a range of plasma parameters. In general, direct interactions of the particle with the mode are required for a measurable loss as shown by examining more than thirty different cases in Fig. 2. Whether the particle directly interacts with the mode is estimated from the separation between the peak location of ECE measured mode amplitude and the location of the guiding center (GC) of the unperturbed orbit at the mid-plane. The data points lying on the negative x side represent cases when the mode is peaking at a radial location further inside than the deepest region the GC orbit reaches at the mid-plane as illustrated by the cartoon on the far left; in this case, the mode is well core-localized. The particles following the typical banana orbit relevant to this AE-induced prompt loss mechanism do not intersect with the mode. Therefore, no coherent prompt loss from this mode is detected at the FILD ($\Delta F = 0$), where ΔF is the coherent loss amplitude at the FILD. On the far right of Fig. 2, the opposite situation is illustrated. The mode is located at a larger radial location and the particle orbit intersects with the mode, leading to loss. RSAEs are generally more core-localized than TAEs, so TAE-induced prompt coherent losses are more often observed than RSAEs. But, if an RSAE has a large amplitude and broad spatial structure which is often the case for low-n modes,[38] it can extend out to intersect with the fast ion orbit and cause prompt loss. This effect explains some of the points with negative x-values but nonzero ΔF in Fig. 2. Other situations in this region (x = 0, $\Delta F \neq 0$) can be explained by the finite gyro radius ($4 \sim 5$ cm). In low plasma current equilibria, however, the banana width of the probing ions can become large enough to probe also the highly core-localized modes as was shown in Fig. 4 of Ref. 20.

The particles are detected only when the phase between the AE and the particle orbit causes an outward displacement (also referred as "kick") that deflects the particles into the FILD, which is why the FILD loss signal is modulated at the

mode frequency. The lost particles traverse the plasma much faster than the mode amplitude evolves. When the mode is stronger in amplitude, it gives the particles a larger kick. Since the FILD is at a fixed location and the ion ionization profile is proportional to the electron density near the plasma edge, the loss rate as measured with the FILD correlates with the mode amplitude. Therefore, there are more particles lost to the FILD at stronger mode amplitude. A linear dependence of the coherent fast-ion flux on the mode amplitude is observed in the experiments, but the slope is different for different modes. The absolute value of the radial displacement (ζ) of the fast ion imparted by each mode can be experimentally inferred using the model given in Eq. (1) of Ref. 21

$$\zeta \approx (\Delta F / \bar{F}) L_i, \tag{1}$$

where $\bar{F}$ is the unperturbed-loss amplitude at the FILD and L_i is the ionization scale length. It has been found that an n = 2 RSAE at mode amplitude ($\delta T_e / T_e$) of 1% can cause a kick as large as 10 cm (for comparison, the typical gyroradius of full-energy beam-ions in these plasmas is $4 \sim 5$ cm). The results enable a novel and quantitative validation of numerical codes. Simulated radial displacements using the full-orbit SPIRAL code with eigenmodes from NOVA agree with the experiments both qualitatively and quantitatively.

B. New experiment setup

New AE-induced prompt loss experiments were conducted, in which the plasma condition, especially plasma current, shape, and gap between last close flux surface (LCFS) and wall are tuned such that the unperturbed (or equilibrium) first orbit of the fast ions from a particular neutral beam will closely approach one of the FILDs. The beam has finite size and centrally (ϕ-z plane) peaked deposition profile. Previous study shows that the sensitivity to perturbations is maximized by selecting the unperturbed orbit to pass through the center of the neutral beam footprint. In these new experiments, the plasma current is ramped up and held at the value for maximum sensitivity. The neutral beam injection is started from $t = 300$ ms during the plasma current ramping; this results in a relatively high fast ion pressure in a reversed magnetic shear plasma,[39] which reproducibly generates Alfvén eigenmodes. As seen in the new experiments, the resultant mode spectra are very similar throughout a series of discharges. Similar to previous measurements,[40] the
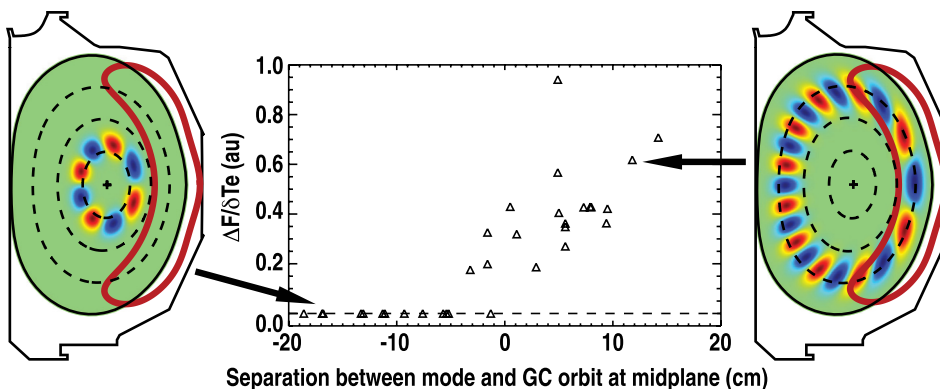

FIG. 2. Energetic particle flux to the FILD for an ensemble of more than thirty cases. Whether there is direct interaction between the particle and the mode is estimated by the separation between the peaking location of the mode amplitude measured by ECE and the guiding center orbit at the mid-plane. Situations with/without coherent loss detection resulting from the orbit with/without direct interaction with the mode are illustrated by the cartoon on the right/left.
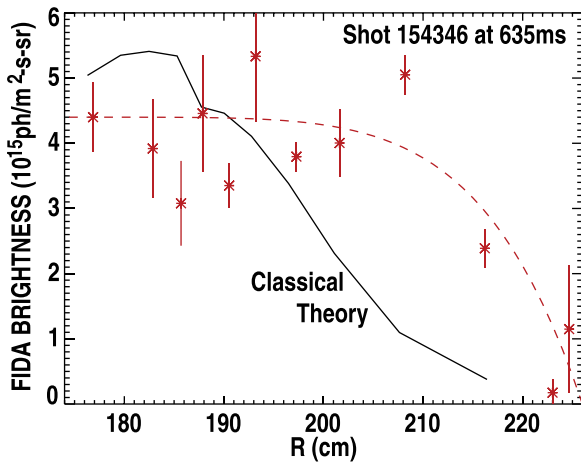
FIG. 3. Fast-ion population profile from vertical FIDA view integrated over 650.5–652.7 nm (Data—asterisks with error bar and fit to data—dashed line) compared to classical prediction (solid line) from FIDAsim calculation.

fast-ion profile is flatter than classically expected [Fig. 3] from FIDAsim[41] calculation and the neutron rate is less than the classical prediction. The beam of interest (for FILD loss detection) is either modulated at 40 Hz or constantly injected with a few beam-off notches. The beam on/off window size of 25 ms (40 Hz) allows loss data from longer time duration and/or from a wider range of mode spectra than in earlier experiments. The beam-off notch for the continuous injection is used as a monitor of the first-orbit loss feature, e.g., rapid rise and decay time of the loss signal in sync with the beam switch on/off. At the same time, the beam-off notch provides data for the $\bar{F}$ measurement. In some discharges, in order to keep the mode spectra unaffected, the reduction of mode drive due to the beam-off notch is compensated with a beam pulse from another neutral beam that does not introduce loss at the FILD.

As Eq. (1) shows, the model predicts that the loss is directly related to the edge ionization rate at the birth location. This has been further verified in the new experiments where gas puff and pellet injection have been utilized to perturb the edge ionization, while minimizing the effects on the equilibrium and the instabilities. Deuterium gas with pulse

durations of 5 ms and 10 ms are puffed into the vessel from the valve located on the top of the machine [Fig. 1]. The ionization rate is proportional to the electron density.[21] As depicted in Fig. 4(a), near the plasma edge ($R \in [2.03, 2.28]$) where the majority of the relevant lost ions are born, the density (and therefore the ionization rate) increases with a 5 ms gas puff in discharge 154 334. The sudden drop in the loss signal at $t = 595\text{–}600$ ms in discharge 154 334 [Fig. 4(b)] is caused by a 5 ms beam-off notch for the beam that supplies the lost particles. The power was compensated by a 5 ms beam pulse from another neutral beam with the same injection geometry at a different toroidal location is utilized to avoid changes in the mode spectra. Since the AE mode activities are similar for plasmas with and without gas puff, fast ions lost to the FILD are originated from the same birth locations. However, the ionization rate at this location is higher in the plasma with gas puff; therefore, the loss at FILD is expected to increase according to the model. As shown in Fig. 4(b), the measured loss with gas puff increases compared to that before the gas puff or from a repeat discharge (154 336) without gas puff, qualitatively consistent with the model. Though the pellet injection introduces a faster and more localized perturbation, the deuterium pellets available for these experiments were too small to make measurable changes to the density.

A wide variety of methods have been used to modulate the amplitudes and structures of the modes, including injection on- and off-axis, perpendicular and parallel injection, co- and counter-injection, changes in neutral beam power, voltage, and timing, and adding electron cyclotron heating (ECH) with different deposition locations.[42] In discharge 154 438, the plasma is heated only by three co-injected neutral beams (30 L, 330 L, and 330 R, named according to their toroidal location and position in the beam housing). The three NBIs are switched on/off simultaneously at 40 Hz [Fig. 5(a)]. The all-beam on/off injection pattern is designed to capture a wider amplitude range of the energetic particle driven modes. As shown in the crosspower spectrum of vertical and radial interferometer [Fig. 5(b)], several TAEs and RSAEs (with frequency up-sweeping) are excited by the sub-Alfvénic beam ions during each 25 ms beam-on window,
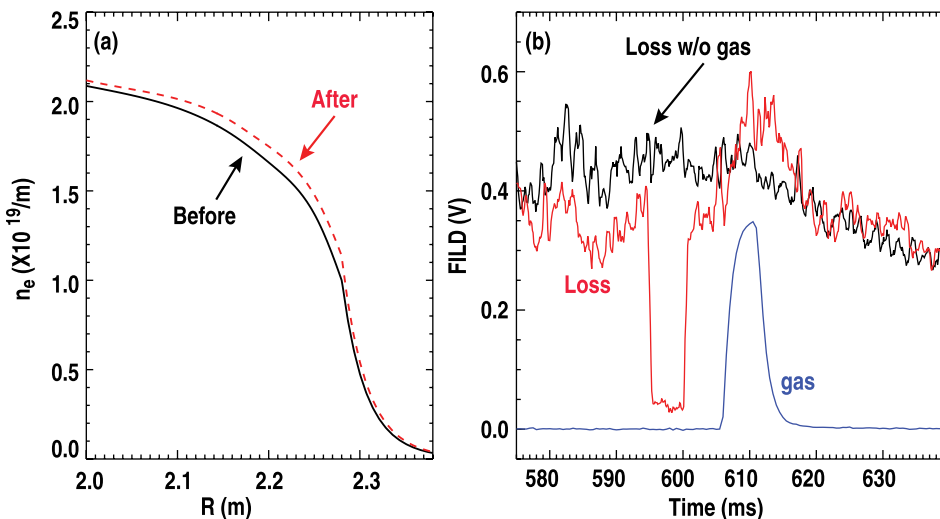

FIG. 4. In discharge 154334, (a) the edge density profile before and after a 5 ms small gas puff [blue solid line in (b)] near 610 ms and (b) the loss signal at FILD in red with the loss signal from comparison discharge 154 336 without gas puff shown in black.
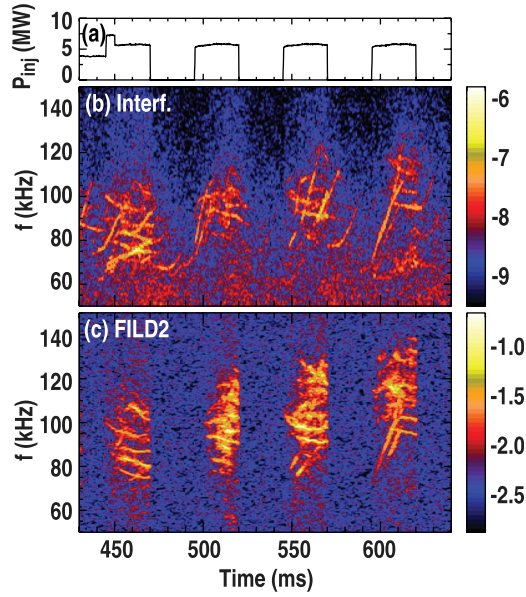
FIG. 5. Time evolution of (a) total neutral beam injected power, (b) spectrogram of cross power between vertical and radial CO_2 interferometers, and (c) spectrogram of FILD2 data in a reversed magnetic shear plasma 154 438.

FIG. 7. Fluctuating FILD loss amplitude ΔF verse the mode amplitudes (ECE measured δTe) for five co-existing TAEs: 75 kHz (red asterisks), 88 kHz (orange diamonds), 95 kHz (blue triangles), and 105 kHz (green squares) between 445–470 ms in discharge 154 438.

while the modes almost vanish once the beams (drive) are turned off. A few RSAEs at low frequencies remain unstable even during the beam-off windows, possibly because they are driven by lower-energy ions in the slowing-down tail. FILD2 detects coherent prompt losses from both TAEs and RSAEs but the TAEs dominate [Fig. 5(c)], as normally found in previous experiments. The loss signal rapidly disappears following the beam-switch-off and reappears with the growing mode amplitudes after the beam-switch-back-on. The FILD2 camera data reveal the loss [Fig. 6(a)] is dominantly from full energy beam ions from 30 L beam and no loss is observed during the beam-off windows [Fig. 6(b)].

The relationship of loss amplitude with the mode amplitude for five TAEs co-existing during the 445–470 ms beam pulse [Fig. 5] is shown in Fig. 7. The frequencies of TAEs vary gradually $\omega_{TAE} \approx \frac{V_A}{2R}\left(\frac{n}{m+1/2}\right) + nV_{rot}$, V_A is the Alfvén speed, V_{rot} is the plasma rotation speed, and R is the major radius, n and m are the toroidal and poloidal mode number, respectively. In Fig. 7, the TAEs are labeled using the average frequency (in the lab frame) during the time interval. Though the TAE radial location moves with the peak of the EP density gradient,[43] the peak electron temperature fluctuations of the four TAEs (75 kHz, 88 kHz, 95 kHz, and
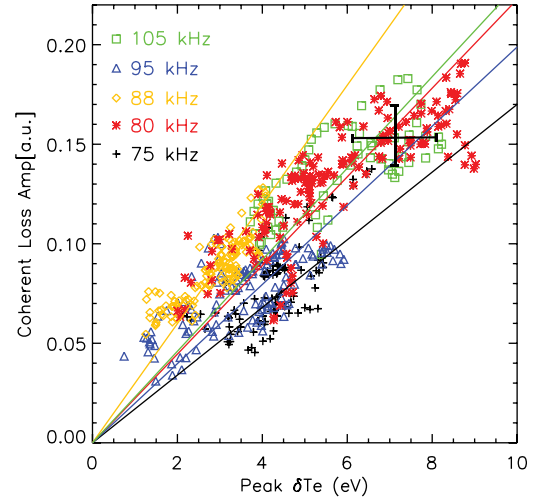
105 kHz) measured by ECE stay in the range of $R = 210$–215 cm in this time interval, while the 80 kHz TAE stays between $R = 205$ and 210 cm. The unperturbed guiding center orbit crosses the mid-plane near $R = 205$ cm and directly intersects with all five TAEs. ECE measurements show that the 88 kHz TAE has the narrowest radial extent. The approximately linear dependence (average exponential fitting of $\sim$0.8) is consistent with previous measurements. Given the complex situation of multiple simultaneous modes, it is not surprising that the correlations are not perfect. Considerations include the temporal variation in transport as other modes impart kicks to fast ions, using the ECE measured δTe as a proxy for the mode amplitude, etc.

A heavy-ion beam probe (HIBP) uses injected ions to probe internal fields in the plasma.[44] Forces on the injected ions due to the modes are manifested as modulated signals at edge detectors. The measurements reported here are conceptually similar to HIBP measurements but have the important advantage that the ion source—the neutral beam injector—is already installed on the tokamak. The second component of the diagnostic technique is one or more (relatively inexpensive) FILDs placed at locations where beam ions born in the edge region on large banana orbits pass close to it after a single poloidal transit through the plasma core. In analogy to the HIBP, we call this new diagnostic technique a LIBP.
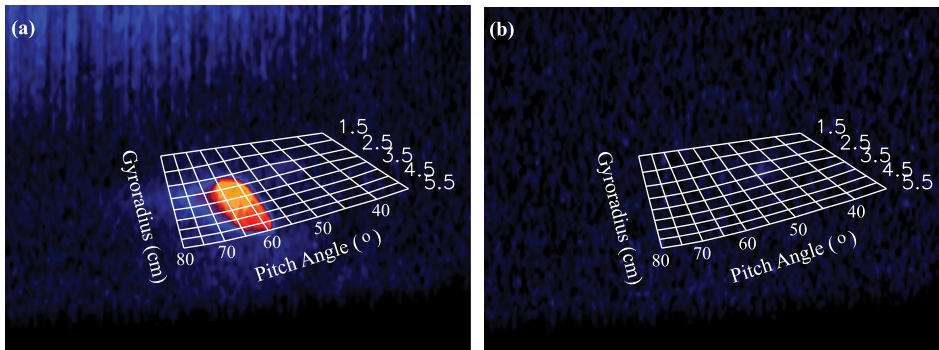

FIG. 6. Camera frame of the FILD2 scintillator at (a) t = 549 ms when 30 L is on, the gyroradius for full energy (81.5 keV) beam ion is $\sim$2.82 cm, (b) t = 541 ms when 30 L is off with calculated mapping grid overlaid in discharge 154 438.

Besides Alfvén eigenmodes, LIBP has also been utilized to probe the plasma response to n = 1 external magnetic perturbation (MP) in recent experiments and analysis is underway.

III. FAST-ION FIRST-ORBIT LOSS THROUGH NON-LINEAR INTERACTIONS WITH MULTIPLE ALFVÉN EIGENMODES

Fast-ion loss measurements in DIII-D show oscillations at the sum, difference, and second harmonic frequencies of two independent Alfvén eigenmodes (first reported in Ref. 24), thereby demonstrating a new non-linear feature of wave-particle interactions.

The additional oscillations are not caused by plasma modes. They are only seen in the particle loss signals not in other fluctuation measurements. An example is shown in Fig. 8., CO_2 interferometer [Fig. 8(a)] and ECE [Fig. 8(b)] measurements show that there are several unstable TAEs and RSAEs in the frequency range of 70–150 kHz in discharge 146 096. The edge magnetic sensor also detects several AEs in the same frequency band [Fig. 8(c)], primarily TAEs and an n = 1 RSAE; the undetected AEs are more core localized with relatively small amplitudes ($\delta B_{peak}/B \leq 1 \times 10^{-3}$). During the time window (340–350 ms) when the neutral beam which generates fast ions that reach FILD2 is switched on, FILD2 detects coherent prompt loss from almost all the AEs detected by interferometers. Interestingly, FILD2 also detects loss at difference and sum frequencies of the n = 4 TAE (128 kHz) and the n = 2 RSAE (103 kHz) (frequencies quoted at t = 345 ms) [Fig. 8(d)].

The non-linearity is also studied through the bi-coherence[45,46] analysis as shown in Fig. 9 for discharge 146 095. The non-linear coupling is evident in the bi-coherence spectrum of the FILD loss signal [Fig. 9(a)], where a high normalized bi-coherence of 0.6 to 0.75 is found at the sum and difference frequencies and at the harmonics of an RSAE (100 kHz) and a TAE (117 kHz). The high bi-coherence

unambiguously confirms the non-linearity. It also strongly supports that these lost particles have interacted with both modes on the short path they took en route to the FILD and the fixed phase relationship (or phase coherence) has not been washed out. At the same time, the absence of bi-coherence in core electron temperature and density fluctuations [Figs. 9(b) and 9(c)] confirms that the two modes are independent from each other and that the non-linear losses are not generated from wave-wave coupling.

These observations reveal a previously unconsidered mechanism by which fusion products may be lost in a reactor. The basic idea is illustrated by the cartoon in Fig. 10, where a particle bounces from one gear to another through a series of kicks by different gears, ultimately making its way to the outside wall. The rate at which particles are kicked out and the location where they hit the wall is a complex combination of each gear's position when the particle reaches it, as well as the initial particle position. In the real experiments, the situations are similar but more complicated. An analytical model is developed to help understand the underlying physics involved. The details of the model can be found in Ref. 23. In the coordinate system of the unperturbed orbit, the particle is deflected by the phase ($\mathbf{k} \cdot \mathbf{r}$) dependent combined force of two independent AEs. (For simplicity, only the electric field components of the modes are considered). When the displacement is small, the orbital displacement r due to the modes can be approximated in an iterative way

$$
\begin{aligned}
r \propto {} & \frac{E_1}{\omega_1^2}\sin(\omega_1 t) + \frac{E_2}{\omega_2^2}\sin(\omega_2 t) + \frac{E_1^2 k_1}{8\omega_1^4}\sin(2\omega_1 t) \\
& + \frac{E_2^2 k_2}{8\omega_2^4}\sin(2\omega_2 t) + \frac{1}{(\omega_1 - \omega_2)^2}\left(\frac{A_1}{\omega_1^2} + \frac{A_2}{\omega_2^2}\right) \\
& \times \sin((\omega_1 - \omega_2)t) + \frac{1}{(\omega_1 + \omega_2)^2}\left(\frac{A_3}{\omega_1^2} + \frac{A_4}{\omega_2^2}\right) \\
& \times \sin((\omega_1 + \omega_2)t) + A_5,
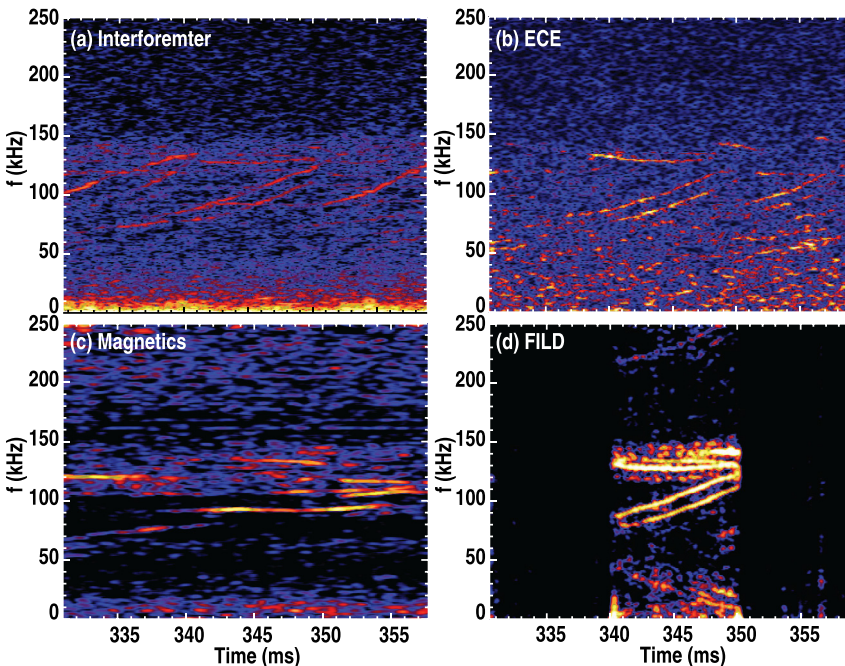\end{aligned}
\tag{2}
$$

FIG. 8. Spectrograms of crosspower of (a) line integrated density signal from CO_2 interferometer R0 and V2 chords, (b) core electron density signal from multiple ECE channels, (c) edge magnetic field signal from magnetic sensors, and (d) spectrogram of fast ion loss signal from FILD2 in discharge 146 096.
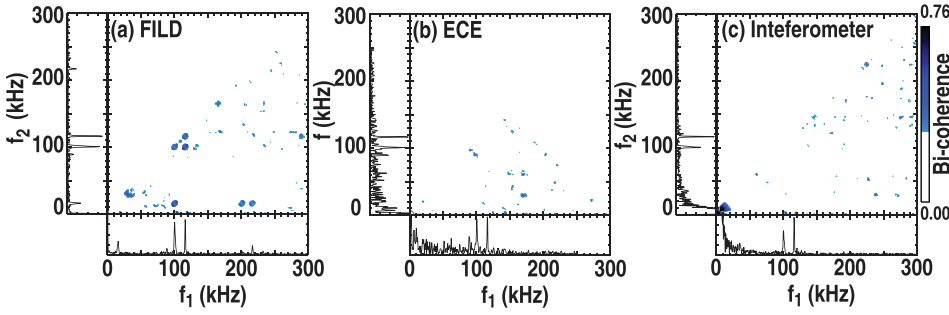
FIG. 9. Bi-coherence of (a) fast ion loss signal from FILD, (b) core electron temperature signal from ECE, and (c) phase measurement of integrated density signal from CO_2 interferometer for discharge 146 095 between 300.4 and 302.2 ms.

where ω, E, and k are the frequency, amplitude, and wave number, respectively, for mode #1 and #2; the A_1–A_5 factors depend on ω, E, k, etc. The model captures many important features of the experiments, such as the additional non-linearly generated difference, sum, and harmonic frequencies, and predicts that the difference term is larger than the sum term, as seen experimentally. To better compare with the experiments, the ionization rate needs to be folded in and factors such as the magnetic perturbations of the modes and the toroidal geometry need to be included. Monte Carlo simulations using the SPIRAL code with NOVA calculated eigenmodes with all these factors included show qualitative agreement with the experiments.[23]

The analytic model and SPIRAL numerical simulations qualitatively explain the FILD frequency spectrum by the non-linear coupling of the fast-ion orbital responses to the two independent AEs. A complete description of the conditions under which the non-linear loss should be detected does not exist yet. Empirically, non-linear features are observed when the AEs are strongly driven, but strong modes do not always generate non-linear loss, as shown in Fig. 11. In discharge 146 096, coherent losses due to a 91 kHz RSAE and a 130 kHz TAEs are detected on the FILD along with losses at the non-linearly generated difference (39 kHz) and sum (221 kHz) frequencies [Fig. 11(c)]. In discharge 146 082, with two TAEs (73 and 90 kHz) [Fig. 11(b)] which have ~2 times higher amplitudes compared to those [Fig. 11(a)] in discharge 146 096, only coherent losses at the fundamental frequencies are detected by the FILD [Fig. 11(d)]. This observation, along with the fact that loss at the difference frequency is higher than loss at the sum frequency, also rules out the possibility of a spurious

FIG. 10. Cartoon showing the influence of one gear on the particle detection at the wall caused by another.

non-linearity introduced by the detector system. The non-linear loss has been observed more often when an RSAE is involved, which is thought to be due to the smaller spatial structure of an RSAE.

IV. SUMMARY AND DISCUSSION

New experiments on AE-induced prompt loss give us new insights into non-resonant prompt losses. The linear dependence of loss amplitude on the mode amplitude is generally observed, for example, the linear scaling is observed for five different co-existing TAEs. The data will contribute to understand how the slope of the linear dependence relates to the mode property such as mode structure, location, and frequency. The method for inferring the radial kick is partially tested in experiments, where small gas puffing is used to perturb the edge density (ionization) profile and the observed coherent increase in FILD loss signal is consistent with the model.

Fast ion losses have been observed at the non-linearly generated sum and difference frequencies of two Alfvén eigenmodes, which are not present on other fluctuation diagnostics. The non-linearity is confirmed by bi-coherence analysis, and it is explained with an analytic model and full orbit simulations by a non-linear interaction between the fast ion and the two AEs. The non-linear process of a single particle being kicked from one wave to the next and ultimately being lost from the plasma, as measured conclusively here, is likely occurring in the simulations presented by White *et al.*[47] for non-resonant and resonant particles alike. His work, however, focused on the larger consequences of multiple modes interacting with the EP population and showed the dominant factor contributing to profile flattening observed in DIII-D experiments is the presence of multiple resonances and overlapping of these resonances.

Further study with the aid of data mining on the non-linear loss from these and other previous experiments will be carried out. In the experiments presented in this paper, the AEs have limited spatial overlap with relatively small amplitudes (barely detected on edge magnetic sensors). There is no wave-wave coupling observed, and therefore, the waves are thought to be independent. Since FILD should be able to measure losses at the beat frequency of two waves which are non-linearly coupled, it will be interesting to see under what conditions wave-wave coupling occurs in the plasma, whether the mode amplitude or the mode spatial overlap plays a more important role, and how FILD loss spectrum differs between wave-wave and wave-particle coupling.
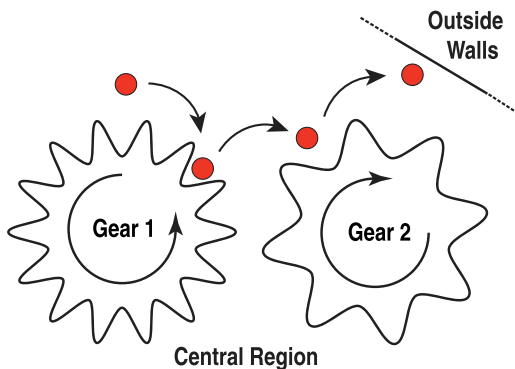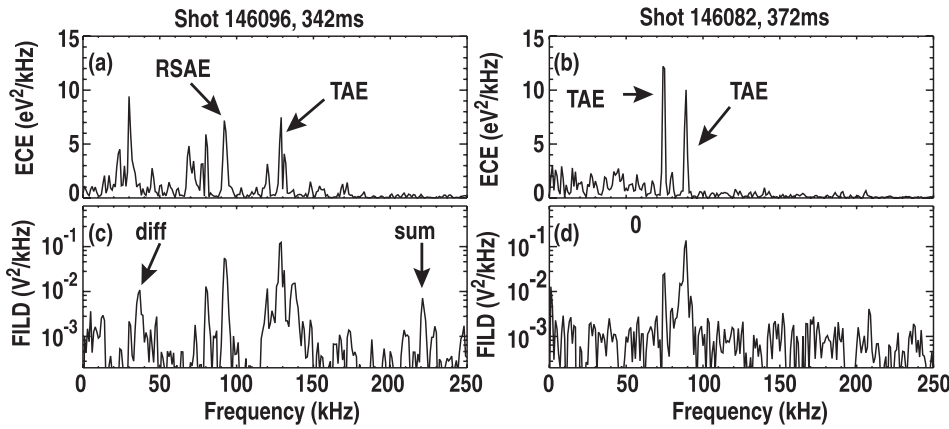
FIG. 11. Spectra of (a) ECE and (c) FILD measurements at $t = 342$ ms in discharge 146 096 and spectra of (b) ECE and (d) FILD measurements at $t = 372$ ms in discharge 146 082.

As demonstrated in Ref. 21, using the full-orbit following SPIRAL and the ideal MHD NOVA codes, the data provide a novel and unique opportunity for quantitative code validation. It will be interesting to apply the data to other orbit and mode calculation codes, for example, using a guiding center orbit code instead of full orbit code, and/or using a mode calculation code which includes self-consistent calculations of mode amplitudes.

ACKNOWLEDGMENTS

[1]W. W. Heidbrink and G. J. Sadler, Nucl. Fusion **34**, 535 (1994).
[2]K. L. Wong, Plasma Phys. Controlled Fusion **41**, R1 (1999).
[3]W. W. Heidbrink, Phys. Plasmas **15**, 055501 (2008).
[4]S. E. Sharapov, B. Alper, H. L. Berk, D. N. Borba, B. N. Breizman, C. D. Challis, I. G. J. Classen, E. M. Edlund, J. Eriksson, A. Fasoli, E. D. Fredrickson, G. Y. Fu, M. Garcia-Munoz, T. Gassner, K. Ghantous, V. Goloborodko, N. N. Gorelenkov, M. P. Gryaznevich, S. Hacquin, W. W. Heidbrink, C. Hellesen, V. G. Kiptily, G. J. Kramer, P. Lauber, M. K. Lilley, M. Lisak, F. Nabais, R. Nazikian, R. Nyqvist, M. Osakabe, C. Perez von Thun, S. D. Pinches, M. Podesta, M. Porkolab, K. Shinohara, K. Schoepf, Y. Todo, K. Toi, M. A. Van Zeeland, I. Voitsekhovich, R. B. White, V. Yavorskij, ITPA EP TG, and JET-EFDA Contributors, Nucl. Fusion **53**, 104022 (2013).
[5]W. W. Heidbrink, M. A. Van Zeeland, M. E. Austin, K. H. Burrell, N. N. Gorelenkov, G. J. Kramer, Y. Luo, M. A. Makowski, G. R. McKee, C. Muscatello, R. Nazikian, E. Ruskov, W. M. Solomon, R. B. White, and Y. Zhu, Nucl. Fusion **48**, 084001 (2008).
[6]D. C. Pace, R. K. Fisher, M. Garcia-Munoz, W. W. Heidbrink, and M. A. Van Zeeland, Plasma. Phys. Controlled Fusion **53**, 062001 (2011).
[7]M. Garcia-Munoz, N. Hicks, R. van Voornveld, I. G. J. Classen, R. Bilato, V. Bobkov, M. Bruedgam, M. Bruedgam, H. U. Fahrbach, V. Igochine, S. Jaemsae, M. Maraschek, and K. Sassenberg, and ASDEX Upgrade Team, Nucl. Fusion **50**, 084004 (2010).
[8]F. Nabais, D. Borba, M. Garcia-Muñoz, T. Johnson, V. G. Kiptily, M. Reich, M. F. F. Nave, S. D. Pinches, S. E. Sharapov, and JET-EFDA Contributors, Nucl. Fusion **50**, 115006 (2010).

[9]E. D. Fredrickson, C. Z. Cheng, D. Darrow, G. Fu, N. N. Gorelenkov, G. Kramer, S. S. Medley, J. Menard, L. Roquemore, D. Stutman, and R. B. White, Phys. Plasmas **10**, 2852 (2003).
[10]N. N. Gorelenkov, H. L. Berk, R. Budny, C. Z. Cheng, G. Y. Fu, W. W. Heidbrink, G. J. Kramer, D. Meade, and R. Nazikian, Nucl. Fusion **43**, 594 (2003).
[11]A. Snicker, E. Hirvijoki, and T. Kurki-Suonio, Nucl. Fusion **53**, 093028 (2013).
[12]C. Z. Cheng, L. Chen, and M. Chance, Ann. Phys. **161**, 21 (1985).
[13]K. L. Wong, R. J. Fonck, S. F. Paul *et al.*, Phys. Rev. Lett. **66**, 1874 (1991).
[14]W. W. Heidbrink, E. J. Strait, E. Doyle, G. Sager, and R. T. Snider, Nucl. Fusion **31**, 1635 (1991).
[15]Y. Kusama, H. Kimura, T. Ozeki, M. Saigusa, G. J. Kramer, T. Oikawa, S. Moriyama, M. Nemoto, T. Fukita, K. Tobita *et al.*, Nucl. Fusion **38**, 1215 (1998).
[16]H. L. Berk, D. N. Borba, B. N. Breizman, S. D. Pinches, and S. E. Sharapov, Phys. Rev. Lett. **87**, 185002 (2001).
[17]S. E. Sharapov, B. Alper, H. L. Berk, D. N. Borba, B. N. Breizman, C. D. Challis, A. Fasoli, N. C. Hawkes, T. C. Hender, J. Mailloux, S. D. Pinches, and D. Testa, Phys. Plasmas **9**, 2027 (2002).
[18]R. K. Fisher, D. C. Pace, M. Garcia-Munoz, W. W. Heidbrink, C. M. Muscatello, M. A. Van Zeeland, and Y. B. Zhu, Rev. Sci. Instrum. **81**, 10D307 (2010).
[19]X. Chen, R. K. Fisher, D. C. Pace, M. Garcia-Munoz, J. A. Chavez, W. W. Heidbrink, and M. A. Van Zeeland, Rev. Sci. Instrum. **83**, 10D707 (2012).
[20]X. Chen, M. E. Austin, R. K. Fisher, W. W. Heidbrink, G. J. Kramer, R. Nazikian, D. C. Pace, C. C. Petty, and M. A. Van Zeeland, Phys. Rev. Lett. **110**, 065004 (2013).
[21]X. Chen, W. W. Heidbrink, G. J. Kramer, M. A. Van Zeeland, M. E. Austin, R. K. Fisher, R. Nazikian, D. C. Pace, and C. C. Petty, Nucl. Fusion **53**, 123019 (2013).
[22]M. Schneller, Ph. Lauber, M. Garcia-Munoz, M. Brüdgam, and S. Günter, J. Phys.: Conf. Ser. **401**, 012022 (2012).
[23]X. Chen, G. J. Kramer, W. W. Heidbrink, R. K. Fisher, D. C. Pace, C. C. Petty, M. Podesta, and M. A. Van Zeeland, "Non-linear wave-particle interactions and fast ion loss induced by multiple Alfvén eigenmodes in the DIII-D tokamak," Nucl. Fusion **54**, 083005 (2014).
[24]L. L. Lao, H. S. John, R. D. Stambaugh, A. G. Kellman, and W. Pfeiffer, Nucl. Fusion **25**, 1611 (1985).
[25]T. N. Carlstrom, D. R. Ahlgren, and J. Crosbie, Rev. Sci. Instrum. **59**, 1063 (1988).
[26]M. E. Austin and J. Lohr, Rev. Sci. Instrum. **74**, 1457 (2003).
[27]T. N. Carlstrom *et al.*, Rev. Sci. Instrum. **63**, 4901 (1992).
[28]L. Zeng, G. Wang, E. J. Doyle, T. L. Rhodes, W. A. Peebles, and Q. Peng, Nucl. Fusion **46**, S677 (2006).
[29]W. W. Heidbrink, Rev. Sci. Instrum. **81**, 10D727 (2010).
[30]C. Z. Cheng, Phys. Rep. **211**, 1 (1992).
[31]M. A. Van Zeeland, G. J. Kramer, M. E. Austin, R. L. Boivin, W. W. Heidbrink, M. A. Makowski, G. R. McKee, R. Nazikian, W. M. Solomon, and G. Wang, Phys. Rev. Lett. **97**, 135001 (2006).
[32]G. J. Kramer, R. V. Budny, A. Bortolon, E. D. Fredrickson, G. Y. Fu, W. W. Heidbrink, R. Nazikian, E. Valeo, and M. A. Van Zeeland, Plasma Phys. Controlled Fusion **55**, 025013 (2013).
[33]C. T. Holcomb, M. A. Makowski, R. J. Jayakumar, S. L. Allen, R. M. Ellis, R. Geer, D. Behne, K. L. Morris, L. G. Seppala, and J. M. Moller, Rev. Sci. Instrum. **77**, 10E506 (2006).

[34] R. J. Goldston, D. C. McCune, H. H. Towner, S. L. Davis, R. J. Hawryluk, and G. L. Schmidt, J. Comput. Phys. **43**, 61–78 (1981).

[35] A. Pankin *et al.*, Comput. Phys. Commun. **159**, 157 (2004).

[36] M. A. Van Zeeland, N. M. Ferraro, W. W. Heidbrink, G. J. Kramer, D. C. Pace, X. Chen, T. E. Evans, R. K. Fisher, M. Garcia-Munoz, J. M. Hanson, M. J. Lanctot, L. L. Lao, R. A. Moyer, R. Nazikian, and D. M. Orlov, Plasma Phys. Controlled Fusion **56**, 015009 (2014).

[37] M. A. Van Zeeland, W. W. Heidbrink, R. K. Fisher, M. García Muñoz, G. J. Kramer, D. C. Pace, R. B. White, S. Aekaeslompolo, M. E. Austin, J. E. Boom *et al.*, Phys. Plasmas **18**, 056114 (2011).

[38] G. Kramer, C. Z. Cheng, Y. Kusama, R. Nazikian, S. Takeji, and K. Tobita, Nucl. Fusion **41**, 1135 (2001).

[39] E. J. Strait, L. L. Lao, M. E. Mauel, B. W. Rice, T. S. Taylor, K. H. Burrell, M. S. Chu, E. A. Lazarus, T. H. Osborne, S. J. Thompson, and A. D. Turnbull, Phys. Rev. Lett. **75**, 4421 (1995).

[40] W. W. Heidbrink, N. N. Gorelenkov, Y. Luo, M. A. Van Zeeland, R. B. White, M. E. Austin, K. H. Burrell, G. J. Kramer, M. A. Makowski, G. R. McKee, R. Nazikian, and DIII-D Team, Phys. Rev. Lett. **99**, 245002 (2007).

[41] W. W. Heidbrink, D. Liu, Y. Luo, E. Ruskov, and B. Geiger, Commun. Comput. Phys. **10**, 716 (2011).

[42] M. A. Van Zeeland, W. W. Heidbrink, R. Nazikian, W. M. Solomon, M. E. Austin, H. L. Berk, N. N. Gorelenkov, C. T. Holcomb, A. W. Hyatt, G. J. Kramer, J. Lohr, M. A. Makowski, G. R. McKee, C. C. Petty, S. E. Sharapov, and T. L. Rhodes, Plasma Phys. Controlled Fusion **50**, 035009 (2008).

[43] Z. Wang, Z. Lin, I. Holod, W. W. Heidbrink, B. Tobias, M. A. Van Zeeland, and M. E. Austin, Phys. Rev. Lett. **111**, 145003 (2013).

[44] T. P. Crowley, IEEE Trans. Plasma Sci. **22**, 291 (1994).

[45] Y. C. Kim and E. J. Powers, Phys. Fluids **21**, 1452 (1978).

[46] Y. C. Kim and E. J. Powers, "Digital Bispectral Analysis and Its Applications to Nonlinear Wave Interactions," IEEE Trans. Plasma Sci. **PS-7**, 120 (1979).

[47] R. B. White, N. Gorelenkov, W. W. Heidbrink, and M. A. Van Zeeland, Plasma Phys. Controlled Fusion **52**, 045012 (2010).